

ADAPTIVE OPTICS WITH THE DEFORMABLE MIRROR NOT IN PUPIL PART 1: EXPERIMENTAL RESULTS (POSTPRINT)

Mala Mateen et al.

**Air Force Research Laboratory
3500 Aberdeen Ave SE
Kirtland AFB, NM 87117**

5 January 2004

Technical Paper

APPROVED FOR PUBLIC RELEASE; DISTRIBUTION IS UNLIMITED.



**AIR FORCE RESEARCH LABORATORY
Directed Energy Directorate
3550 Aberdeen Ave SE
AIR FORCE MATERIEL COMMAND
KIRTLAND AIR FORCE BASE, NM 87117-5776**

Adaptive Optics with the Deformable Mirror not in Pupil - Part 1: Experimental Results

Mala Mateen^a, Darryl Sanchez^a, Troy Rhoadarmer^b, Loretta Arguella^c, Denis W. Oesch^d, Deborah Fung^b, Roger Petty^c, Patrick Kelly^a, R. Anthony Vincent^a, Jeff Richey^a

^aAir Force Research Lab, 3550 Aberdeen Ave SE, Kirtland AFB, NM

^bSAIC, Lasers & Imaging Technology Lab, 1833 Sunset Place, Suite A
Longmont, CO 80501

^cBoeing-LTS, PO Box 5670, Kirtland AFB NM

^dSAIC, 2109 Air Park Rd. S.E. Albuquerque, NM 87106

December 03, 2007

ABSTRACT

This is the first of two papers discussing aspects of placing the deformable mirror in a location not conjugate to the pupil plane of the telescope.

The Starfire Optical Range, Air Force Research Lab is in the process of developing a high efficiency AO system for its 3.5 m optical telescope. The objective is to achieve maximum diffraction limited performance, i.e., largest pupil diameter possible, and maximum optical throughput. The later can be achieved by placing the deformable mirror outside the pupil. However placing the DM in a location not conjugate to the pupil results in a degradation in optical performance. This paper discusses experimental measurements of the degradation.

In this paper we discuss the DM-not-in-pupil experimental testbed, the difficulties associated with creating this type of testbed, and how these difficulties were overcome. We also present results from the successful lab demonstration of closed performance with the DM placed out of pupil. We experimentally measured the degradation in Strehl and implemented a mitigation technique. Our experimental results indicate the mean degradation in Strehl as a result of placing the DM out of pupil to be between 7 % and 9 %. This result is comparable with wave optics simulation and theoretical results which will be discussed in a companion paper, “Adaptive optics with DM not in pupil - Part 2: Mitigation of Degradation”.

1. INTRODUCTION

The adaptive optics systems of more and more telescopes are placing the deformable mirror out of pupil for a variety of different reasons ranging from the need to perform multi-conjugate adaptive optics (MCAO) to the need to minimize the number of optical surfaces in order to improve throughput. An innovative approach used by some telescopes converts the secondary

mirror into a deformable mirror (DM). An adaptive secondary provides maximum sensitivity at wavelengths longer than $2\mu\text{m}$ making it particularly suitable for thermal infrared astronomy where there is a need to limit the number of warm surfaces involved in adaptive correction. For infrared astronomy an adaptive secondary is also attractive for MCAO since the secondary is roughly conjugate to the strong ground layer.^{1,2} A few examples of telescopes with adaptive secondaries is given below.

The 6.5 m Multiple Mirror Telescope (MMT) at Mt. Hopkins in Southern Arizona is the first in the world to use an adaptive secondary^{3,4} for wavefront sensor correction. Placing the DM at secondary in this case allows for higher throughput, lower emissivity, and a simpler optical setup. Miller et al. 2004⁴ report the measured Strehl to be 40 % of the diffraction limited peak.

The Large Binocular Telescope (LBT) on Mt. Graham, Arizona has two 8.4 m primary mirrors and two 0.91 m Gregorian secondary mirrors. The secondary mirrors are the deformable mirrors for the LBT adaptive optics system.¹ The DMs for the LBT were designed based on the successful MMT adaptive secondary design. The Very Large Telescope (VLT) at Paranal, Chile will upgrade one of the 8 m telescopes to include a deformable secondary mirror (DSM).⁵

The Starfire Optical Range (SOR) is developing a high-efficiency AO system for the 3.5 m telescope. In order to maximize throughput the number of surfaces between the primary mirror and the science camera have to be minimized. The proposed configuration places the DM 1 km behind the 3.5 m primary mirror in output space (see Fig. 1).

We built an AO testbed to test closed loop performance in the DM-not-in-pupil (DNiP) configuration. The experiment consists of two beam injections with the beacon effectively observed at $\approx 90 - 100$ km and the science object at higher elevations (see Fig. 2). The wavelength of the science and the beacon beams was scaled to 589 nm. The optical design allowed for the DM to be moved in and out of pupil. For the experiment presented here we placed the DM ≈ 1 km behind the pupil. The beacon is used to correct the science object which leads to missampling of the atmosphere. We have the problem of correcting the atmosphere at the beacon altitude and applying that correction to the science beam at the science altitude. This leads to degradation in Strehl which is also seen in the wave-optics simulations done by Dr. Barry Foucault.⁶ The simulations show $\approx 7\% - 15\%$ degradation in strehl as the DM is moved 1 km out of pupil. The theoretical cause of degradation in Strehl and the simulation results showing degradation will be discussed in, Adaptive optics with DM not in pupil - Part 2: Mitigation of Degradation,⁷ from here on referred to as Part 2.

In section 2, we present background detailing the DM-not-in- pupil (DNiP) geometry under which the problem arises. In section 3 we discuss the optical design which allowed us to, create a two beam injection with the beams originating at different altitudes, move the DM relative to the pupil, have both the beams scored on and measured in pupil and out of pupil. In Section 4 we present and discuss our experimental results. In section 5 we present results from the experimental implementation of a mitigation strategy. In section 6 we conclude our findings on closed loop Strehl performance with DNiP.

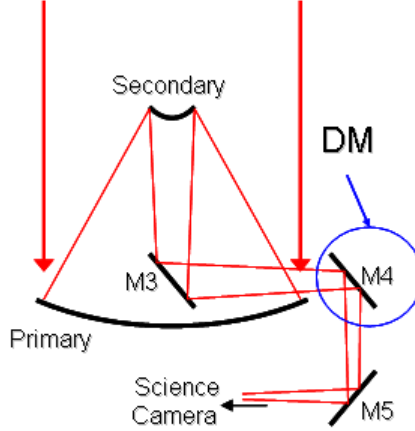


Figure 1. *DNiP geometry side view*

2. BACKGROUND

The astronomical community relies heavily on imaging of astronomical objects to conduct their science. In the optical regime these images are corrupted by the atmosphere. For optical imaging, the object chosen is generally close to zenith making the turbulence path short, which implies low scintillation, i.e. $\sigma_\chi^2 < 0.2$ and moderate isoplanatic angles, $\theta_0 \sim 7\mu rad$. As such, the disturbance is an irrotational, phase-only field near the pupil of the telescope. Conventional adaptive optics^{8,9} corrects this irrotational, phase-only field and creates a sharp image of the science object.

If the imaged object is a point source, then its true phase is known to be flat and hence all phase aberrations on the beam are induced by the atmospheric turbulence. Hence, stars can serve as beacons for the AO system, but the number of stars bright enough to act as a beacon is limited and this fundamentally limits the sky coverage with NGS systems. Laser guide stars (LGS) partially alleviate this restriction and they come in two types, Rayleigh beacons or sodium beacons. In both cases, these beacons are formed within the atmosphere and so are at finite conjugates.

When imaging an astronomically interesting object at infinity and using a beacon at a finite conjugate to correct for it, AO correction suffers from what is called focus anisoplanatism. Focus anisoplanatism refers to the degradation in Strehl that results because the beacon and science beams sample different atmospheres, for instance, a sodium LGS which creates the beacon by exciting sodium atoms in the sodium layer at 90 – 100 km at zenith, will sample a cone of atmosphere with its apex at 90 – 100 km. The science object, on the other hand, may be at ∞ hence traverses a cylinder of atmosphere (see Figure 2). Since the science signal is corrupted by a slightly different atmosphere than the beacon and the LGS is used to correct the science beam's phase, this leads to focus anisoplanatism.

If maximum diffraction limited performance is required, i.e. largest pupil diameter possible, and if maximum optical throughput is required, then one approach is to place the AO system

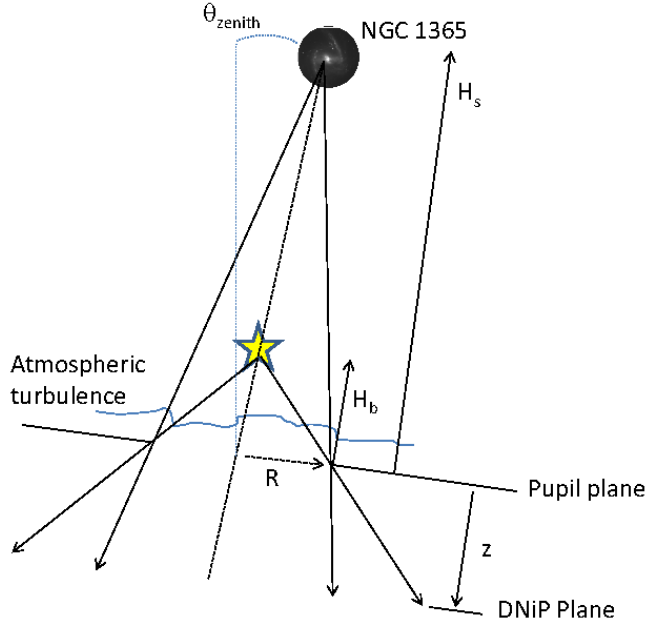


Figure 2. *Geometry of focus anisoplanatism. The height of the Na Guide star (beacon) is H_b and that of the science object is H_s . R is the aperture radius and the DM is placed a distance z behind pupil. Note the different atmospheres traversed by the two beams leading to focus anisoplanatism. Also note the difference between the beacon and science beams at distance z from the pupil plane.*

on gimbal and it is highly desirable to replace an on-gimbal mirror with the DM. When this is done, the DM is no longer in the pupil. Placing the DM out of pupil in this manner results in an additional error due to beam magnification. In keeping with standard naming conventions we call this error, ‘magnification anisoplanatism’. Wave optics simulation of the DNIP geometry found the degradation in Strehl to be $\sim 7 - 15\%$.⁶ A further degradation in Strehl is caused due to the Fresnel propagation of an aberrated wavefront as well as the degradation due to focus anisoplanatism from the pupil to the DNIP plane. Simulations show the degradation due to Fresnel propagation to be less than 1 % (see appendixA). The degradation due to the propagation of focus anisoplanatism is shown to be less than 0.7 % in simulations for our set-up. In Part 2 we theoretically explore the cause for the degradation in Strehl as a result of the DNIP geometry and suggest theoretical mitigation techniques to recover the Strehl. We also discuss magnification anisoplanatism, and the simulations done degradation due to propagating focus anisoplanatism. For this paper we experimentally explored the cause and effect of the degradation in Strehl and experimentally implemented a mitigation technique.

3. DM-NOT-IN-PUPIL OPTICAL DESIGN

In this project we experimentally explored the effects of having a single DM not conjugate to the pupil. Below we describe the AO design for DM-not-in-pupil including how we achieved the

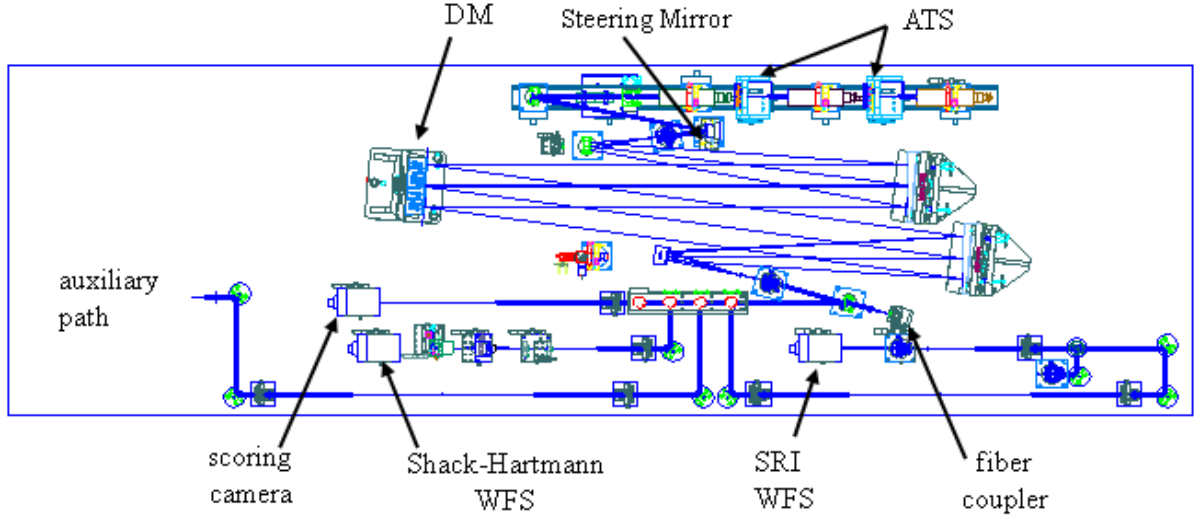


Figure 3. *The basic adaptive optics design in the ASALT lab has the SM, DM, SRI WFS, and Shack-Hartmann WFS conjugate to each other and the DM defines the pupil.*

proper magnification in the experimental setup.

The Atmospheric Simulation and Adaptive Optics Lab Testbed (ASALT) facility at the SOR provides a flexible architecture and a well controlled environment, ideal for this kind of testing. The basic ASALT AO design shown in Figure 3 consists of a $1550\,\mu\text{m}$ laser beam injection. A two-layer atmosphere is simulated using an Atmospheric Turbulence Simulator (ATS) which uses static phase plates imprinted with Kolmogorov statistics and is capable of generating a wide range of atmospheric conditions. The phase plates are located in the middle of two, back-to-back afocal systems. By placing the phase plates in converging portions of the beam, the magnitude of r_0 can be controlled by moving the plates up or down the beam path. In addition, scintillation can be controlled by selecting appropriate field lenses for each afocal system to adjust the effective altitude of the turbulence. Greenwood frequencies are adjusted by rotating the phase plates through the optical beam by computer-controlled stepper motors.¹⁰ A Steering Mirror (SM) is used to correct tilt on the optical beam, a DM to correct higher order aberrations, and wavefront sensors (WFSs) to sense the wavefront aberrations. The wavefront can be measured with a Self Referencing Interferometer (SRI) or a Shack-Hartmann WFS. In addition there is an auxiliary path which allows additional sensors. The SM, DM and wavefront sensors are conjugate to each other and the physical aperture at the DM defines the pupil.

For the DNiP optical design to be added, three main changes to the basic optical bench were implemented. 1) The ATS input was converted to allow for injection of two sources, one for the signal and one for the beacon. Polarization isolation was used to distinguish between the beams and the relay optics before the scoring camera were adjusted so that both the sources could

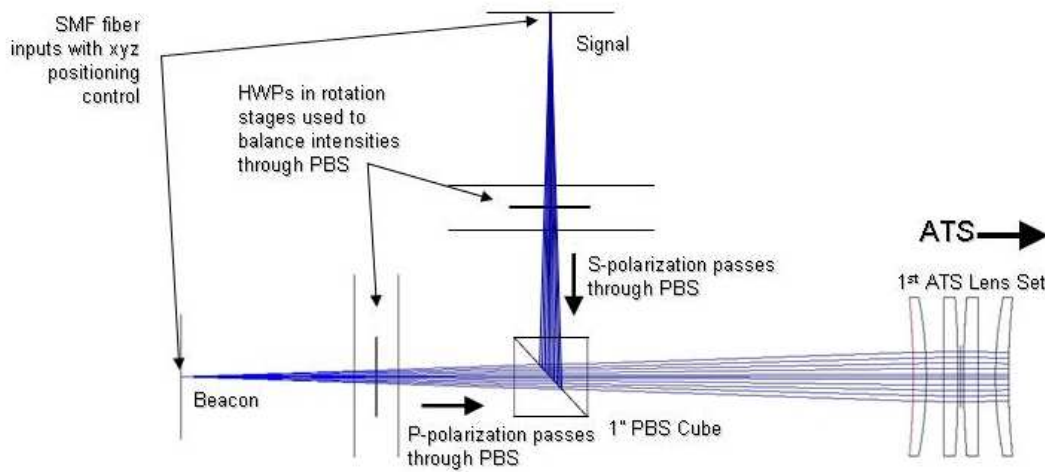


Figure 4. *The schematic shows the 2 beam injection using half-wave plates and Polarizers.*

be optically separated and individually focused on the scoring camera. 2) Opto-mechanical modifications were made to place the pupil aperture in a location in front of the SM. This allows the pupil to be arbitrarily placed relative to the DM and would maintain the relationship between the SM, DM and the WFSs. 3) A second SRI WFS was placed in the auxiliary path to observe the wavefront at the pupil whenever the pupil was not conjugate to the DM.

The design used three wavefront sensors, two SRI WFS and one Hartmann WFS. One SRI WFS referred to as SRI 1 is conjugate to the DM, the second SRI WFS referred to as SRI 2 is conjugate to the pupil. The Hartmann WFS was conjugate to the DM plane.

3.0.1. Two-Beam Injection

The ATS for the basic AO design is configured with a single injection fiber for a combined beacon and signal source. However the DNIP concept requires two independent sources that originate at different altitudes and diverge to different diameters beyond the aperture. Therefore the ATS fiber injection was modified to incorporate a 2 beam injection with xyz stages to control source relative sky positions. The beacon beam is collimated coming out of the ATS and the signal beam slightly converges to represent higher altitudes. The beams model a scenario in which the the Na layer or the beacon is at 90 km at a zenith angle of 45 deg and the signal originates at a higher altitude. Polarizers were used to separate the beams and allow isolation at the different WFSs. The two-beam injection concept is demonstrated in figure 4 and the hardware for the two-beam injection is shown in figure 5.

3.0.2. Optical Trombone

An optical trombone was introduced to create an accessible pupil after the ATS so that the SM, DM and WFSs could be moved relative to the pupil. To accomplish this the turning flat that

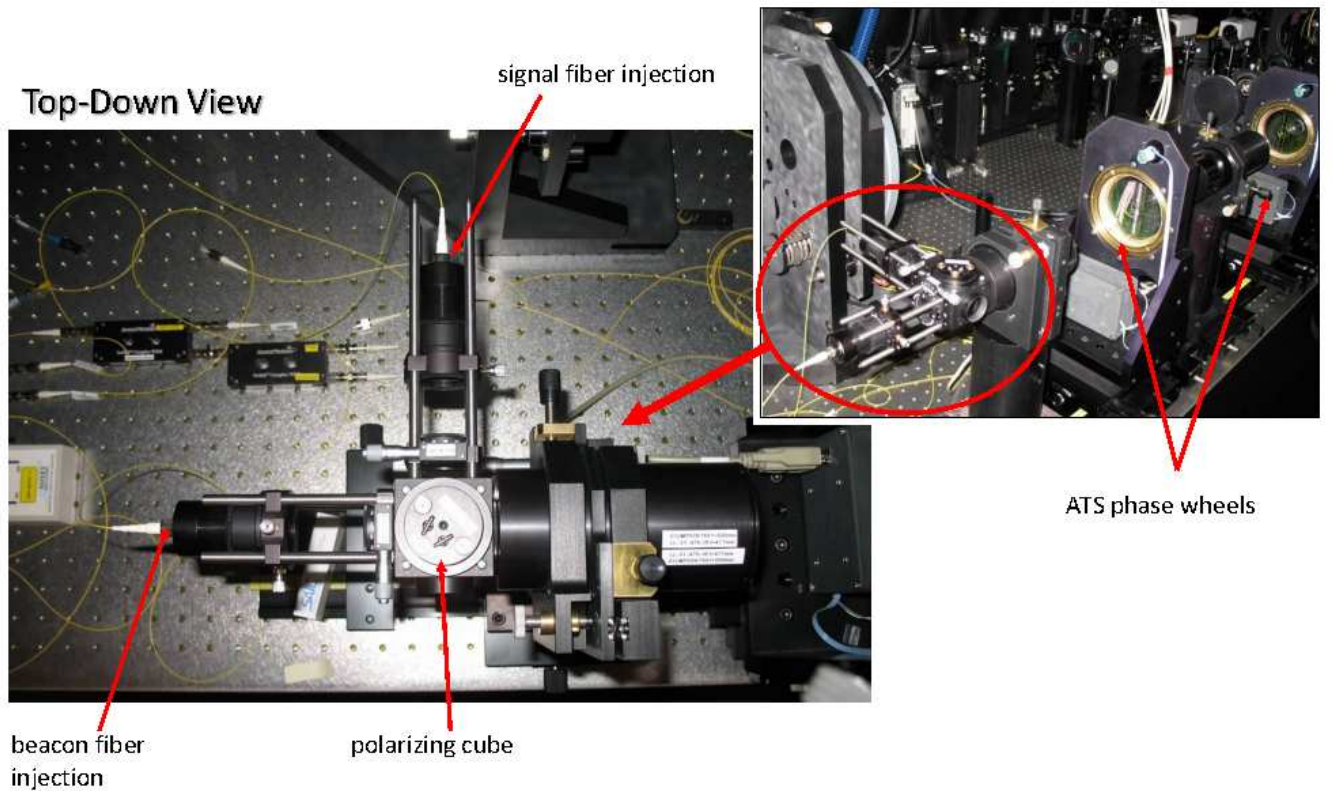


Figure 5. *The hardware mounts used for the 2 beam injection.*

reflects light coming from the ATS to the SM was removed. Instead the light was allowed to pass to an optical trombone which controlled the path length between the new pupil and the SM which is conjugate to the DM and WFSs (see figure 6). Adjusting the length of the trombone controls the location of the DM relative to the pupil. An afocal relay directs the beam back into the optical system at the SM. The experiment was Fresnel scaled for an aperture size of 3.5 m, science wavelength of 850 nm, beacon wavelength of 589 nm, and for placing the DM 1 km out of pupil.

3.0.3. Two-Beam Scoring

The science and beacon beams were scored separately on the same Scoring camera so that point spread functions for both beams could be determined with minimal bias. Polarizing beam splitters were used to separate the science and beacon beams along different paths which could be adjusted for focus on the scoring camera. Linear Polarizers placed in front of each WFS allowed beam selection for measurement.

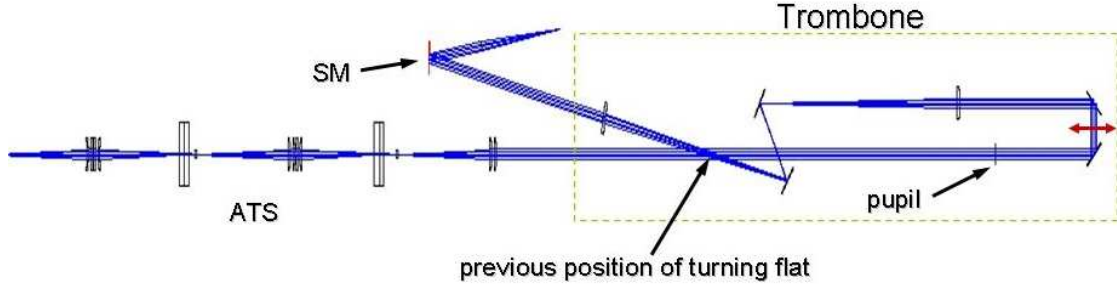


Figure 6. The turning flat was removed to allow the beam to pass to the optical trombone which controls the path length between the new pupil and the SM. Adjusting the length of the trombone controls the pupil position relative to the DM.

3.1. Optical Design Constraints

The purpose of the DNiP optical design was to experimentally evaluate the degradation in Strehl caused by moving the DM ~ 1 km out of pupil or to the z_{DniP} plane. As designed SRI 1 and the Hartmann WFSs are conjugate to the z_{DniP} plane. SRI 2 is conjugate to the pupil plane and measures the wavefront as seen at the pupil. The objective was to measure the wavefront at the pupil plane and at the DNiP plane and compare the difference in Strehl.

Strehl is measured by taking the ratio of an aberrated beam with respect to the diffraction limited point spread function (PSF). To measure the PSF a clean beam is needed which is traditionally provided with the help of a pop-up which injects a beam into the system after the ATS and passes it to the SM, DM, and WFSs. This way any aberrations which may creep in due to light hitting the edge of the phase wheels is avoided, any beam distortions due to faulty alignment of the ATS is also avoided. To make room for the new turning flat position and the optical trombone (see figures 3 and 6) the ATS pop-up had to be removed. Therefore we no longer correct for the above mentioned aberrations.

Ideally a comparison of the SRI 1 and SRI 2 WFS data would show the degradation in Strehl. However a one-to-one comparison of SRI 1 data to SRI 2 data could not be made. SRI 1 and the DM are conjugate but out-of-pupil and in the z_{DniP} plane. SRI 1 senses the wavefront in the z_{DniP} plane and the DM which performs AO corrections is also in the z_{DniP} plane. However SRI 2 senses the wavefront at the pupil plane and the DM which applies AO corrections is at the z_{DniP} plane. Therefore a one-to-one comparison of the corrected wavefronts sensed at SRI 1 and SRI 2 could not be made.

The optical trombone can be adjusted to move the pupil relative to the DM however as the pupil moves the effective atmosphere mapped onto the DM propagates. When the DM is effectively moved 1 km out of pupil the atmosphere it sees also propagates 1 km beyond the pupil.

Therefore a strictly one-to-one Strehl comparison between the DM-in-pupil to a DM-out-of-pupil is not possible; the Fresnel propagation of turbulence has to be accounted for.

3.1.1. Solution to Optical Constraints

The optical design obstacles faced were overcome by properly processing the data. We will address how this was done for each optical design constraint in turn.

The lack of an ATS pop-up (see section 3.1) prevented us from obtaining a diffraction limited spot and from determining the ideal PSF. This left us with only the option of passing the signal beam through the puck* in the phase wheels to record the true PSF. The Strehl measured by comparison with the ideal PSF therefore may be artificially lowered. However this effect shows up in both DM-in-pupil and DM-not-in-pupil measurements, and since we are only interested in the Strehl comparison of the two, the comparison should be unaffected by an imperfect PSF.

As explained in section 3.1, data from SRI 1 and SRI 2 WFSs cannot be compared since one of them is conjugate to the DM and the other is not. To get around this problem we go through the following reasoning: for the beacon beam which is collimated beyond the ATS (see section 3.0.1) the Strehl measured at the pupil plane and at the z_{DNiP} plane should be similar. The only difference between the two should be due to Fresnel propagation of the phase which causes less than 1 % degradation in intensity at the aperture edges (see appendix). Since the beacon beam is collimated there will be no degradation due to magnification anisoplanatism. Therefore the beacon Strehl measured with DM at pupil is identical to the beacon Strehl measured with DM ~ 1 km out of pupil. If the phase screens are placed at pupil than we can approximate the science Strehl at pupil to the beacon Strehl at pupil which is in turn equal to the beacon Strehl at the z_{DNiP} plane (see table below). If we assume all the phase is at the aperture than the beacon and science beams do not suffer from focus anisoplanatism. We show in Part 2 that this degradation is negligible in the DNIP geometry, therefore this assumption is valid. And at the pupil plane they will not suffer from magnification anisoplanatism. We thus conclude that $\text{Beacon}_{pupil} \text{ Strehl} = \text{Beacon}_{z_{DNiP}} \text{ Strehl} = \text{Science}_{pupil} \text{ Strehl}$. This allows us to determine the effective calculation of the science Strehl at pupil.

In order to measure the DNIP degradation we compare the science Strehl at pupil with the science Strehl at the DM or z_{DNiP} plane. In the DNIP set-up the SRI 1 and the DM are conjugate to one another and effectively about ~ 1 km out of pupil, therefore we measure the science Strehl at the z_{DNiP} plane while correcting on the beacon beam. Now we have the effective calculation of the science Strehl at pupil (see No. 3 in Table 1) and the measurement of the science Strehl at the z_{DNiP} plane (see No. 4 in Table 1). The comparison of the two allows us to determine the degradation in Strehl that results when the DM-WFS pair are moved ~ 1 km out of pupil.

A drawback of this approach is that when effectively measuring the science beam at pupil we correct on the science beam instead of the beacon whereas in experiments where the LGS is used, wavefront correction is done using the Na beacon and not the science object. When using the science beam to wavefront correct instead of the beacon we are unable to account for

*The phase wheels are imprinted with Kolmogorov statistics capable of generating a wide variety of turbulence conditions. A hole is cut out from the center of the phase wheels to allow a clean unaberrated beam to pass through. This cut out is referred to as the puck and is used to record a true PSF.

No.	Scoring Beam	WFS		DM plane
		source	plane	
1	beacon	beacon	pupil	pupil
2	beacon	beacon	$z_{DNI\bar{P}}$	$z_{DNI\bar{P}}$
3	science	science	pupil	pupil
4	science	beacon	$z_{DNI\bar{P}}$	$z_{DNI\bar{P}}$
5	science	beacon	pupil	pupil

Table 1. *If the beacon beam is collimated, then the beacon Strehl measured at pupil equals the beacon Strehl measured at the $z_{DNI\bar{P}}$ plane. If all the turbulence is at the pupil then science Strehl at pupil equals the beacon Strehl at pupil which in turn equals the beacon Strehl at the $z_{DNI\bar{P}}$ plane. Thus by measuring the beacon Strehl at the $z_{DNI\bar{P}}$ plane we can determine the science Strehl at the pupil plane strictly assuming all the turbulence is at the pupil. By way of this logic case No. 1 = No. 2 = No. 3. No. 4 is the measurement of the science beam at the $z_{DNI\bar{P}}$ plane while being corrected on by the beacon beam. No. 5 is the measurement of the science beam at the pupil plane while being corrected on by the beacon beam.*

focus anisoplanatism but this is not a significant concern since focus or cone anisoplanatism is a well known and well quantified degradation; and propagation of cone anisoplanatism 1 km out of pupil causes a degradation in Strehl of less than 0.7 % for a 3.5 m aperture where the 589 nm beacon beam originates at an altitude of ~ 90 km and the science object is at a relatively higher altitude (see Fig. 2).

4. EXPERIMENTAL RESULTS

From May 2nd to August 6th 2007, 17 data runs were made, 14 of which were taken in the DNI \bar{P} configuration and 3 in the All-in-pupil (AiP) configuration (see Table 2). The initial data sets were to check that the optical design was implemented properly, to make sure both beams could be scored on, and to ascertain if the science beam had the correct amount of curvature when viewed at the SRI 2 WFS or the pupil WFS.

Data Collection Summary						
Date	Configuration	ATS field lenses [△]	LPW position (cm)	HPW position (cm)	Data Runs	Purpose
05/02/2007	DNiP	4	107.5	54.6	1	a,b,*
05/03/2007	DNiP	4	106.0	52.0	1	a,c,*
05/04/2007	DNiP	4	105.2	52.3	1	a,*
05/08/2007	DNiP	4	105.0	55.0	1	a,d,*
05/10/2007	DNiP	21	107.7	56.7,57.7	1	a,e,*
05/11/2007	DNiP	21	107.7	56.7,57.4,57.1,57.7	6	e,f,*
05/23/2007	DNiP	21	107.7	57.4	5	e,f,○
05/24/2007	DNiP	21	107.7	57.4	5	e,f,○
05/29/2007	DNiP	21	107.7	57.4	5	e,f,○
05/30/2007	AiP	21	107.3,107.7	57.2,57.4	2	e,f,○
05/31/2007	AiP	06	99.3,100.0	56.7, 56.9	4	e,f,○,◇
06/01/2007	AiP	06	99.3	56.7	2	e,○
06/20/2007	DNiP	06	99.3	56.7	5	e,○,◇
06/27/2007	DNiP	06	99.3	56.7	—	○,◇
06/29/2007	DNiP	06	99.3	56.7	8	e,g,○,◇
08/03/2007	DNiP	06	99.3	56.7	1	e,h,○,◇
08/06/2007	DNiP	06	99.3	56.7	1	e,h,○,◇

Table 2. *a) system check. b) create phase reference files for Hartmann & SRI WFS. c) comparison of the Hartmann & SRI phase reference to assign scaling for the DM. d) created system flat map from DM flat map. e) data acquisition. f) experimentally determine curvature on the science beam by measuring it on the pupil-SRI. g) Beam clipping on south-west side of the WFSs. h) score on science beam while measuring first beacon beam and then science beam on DM-SRI. △ See section 3 for description of ATS field lenses. * Low altitude phase wheel (LPW) = 16 B, high altitude phase wheel (HPW) = 32 B. ○ LPW = 16 B, HPW = 16 C. ◇ tracking problems.*

4.1. DM-Not-in-Pupil Configuration

In the DNiP configuration the DM, SM and SRI 1 are conjugate to one another and ~ 1 km out of pupil. The degradation in Strehl is determined as the DM-SRI 1 WFS pair is moved out of pupil. Details of how the DM-SRI 1 WFS pair is effectively moved out of pupil and exactly how the comparison in Strehl is made are given in section 3.1.1 and illustrated in Table 1. On June 29, 2007 we determined the DNiP Strehl by carrying out 8 identical closed loop experiments. The atmospheric parameters under which the tests were conducted are, coherence length $r_0/d = 3.8$, Rytov = 0.1, and Greenwood Frequency $f_g = 98$ Hz for PW speed of 5 steps/revolution and $f_g = 235$ Hz for 12 steps/revolution.

For all the given atmospheric parameters tested, we first perform a baseline measurement which was equal to configuration No. 2 of Table 1. We measured the beacon wavefront at SRI 1, corrected on the beacon beam and scored on the beacon beam. Since configuration No. 2 is equal to configuration No. 3 of Table 1 we are effectively able to determine the intensity of the science beam at pupil (see 3.1.1).

In order to measure the intensity of the science beam ~ 1 km out of pupil we took data in the DNiP configuration. We measured the science wavefront at SRI 1, used the beacon measured at SRI 1 to correct the wavefront and scored on the science beam i.e. we carried out experiment configuration No. 5 of Table 1.

For both cases, configurations No. 3 and No. 5 of Table 1, the beams were first propagated through non-turbulent space in order to obtain the ideal PSF or diffraction limited spot. Then turbulence was introduced and the aberrated beams were sensed at the wavefront and corrected through a closed loop operation. The aberrated PSF is divided by the ideal PSF to obtain the Strehl. A comparison of the Strehl obtained from experiment configurations No. 3 and No. 5 of Table 1 allowed us to determine the degradation in Strehl as the DM-WFS pair was moved ~ 1 km out of pupil. The degradation in Strehl determined for the 8 different data runs referred to as cases was done on June 29th 2007 and is given in Table 4.

June 29 2007 Data — Lens set 6							
LWP = 16B, HWP = 19C, both PWs in pupil							
PW rotation speed 5, 5							
$D_g = \frac{SRI\ 1\ bcn - SRI\ 1\ sci}{SRI\ 1\ bcn} * 100$				Statistics			
Case 1	Case 3	Case 5	Case 8	Mean $_{D_g}^{1,3,5,8}$	Std $_{D_g}^{1,3,5,8}$	Mean $_{D_g}^{3,5,8}$	Std $_{D_g}^{3,5,8}$
(%)	(%)	(%)	(%)	(%)		(%)	
2.82	8.89	7.78	9.43	7.23	3.02	8.70	0.84
PW rotation speed 12, 12							
$D_g = \frac{SRI\ 1\ bcn - SRI\ 1\ sci}{SRI\ 1\ bcn} * 100$				Statistics			
Case 2	Case 4	Case 6	Case 7	Mean $_{D_g}^{2,4,6,7}$	Std $_{D_g}^{2,4,6,7}$	Mean $_{D_g}^{4,6,7}$	Std $_{D_g}^{4,6,7}$
(%)	(%)	(%)	(%)	(%)		(%)	
-7.0	2.09	3.16	3.37	0.41	4.97	2.87	0.69

Table 3. *The science Strehl measured with DM-WFS in the z_{DNiP} plane is compared to the science Strehl measure when the DM-WFS pair is conjugate to pupil. SRI 1 bcn refers to the beacon Strehl measure with the SRI 1 WFS and SRI 1 sci refers to the science Strehl measure with the SRI 1 WFS. The different cases correspond to the repeated data runs done to reduce the error. Cases 1, 3, 5, & 8 were done under the same turbulence conditions, the PW rotation speed was 5 steps/revolution corresponds to $f_g = 97$ Hz. For cases 2, 4, 6, & 7 the simulated turbulence was stronger relative to the previous cases; the PW rotation speed of 12 steps/revolution corresponded to $f_g = 235$ Hz.*

In cases 1, 2, 4, 6, and 7 we encountered tracking problems. Instead of closing the track loop on the beacon beam the system was closing on the science beam. Since both the beacon and science beams were scored on the same camera in a 128 by 128 pixel box it is possible that for cases 2, 4, 6, and 7 the speckle was high enough to cause the aberrated beacon and science beams to overflow into one another thus confusing the centeroiding algorithm and causing it to track on the science spot instead of the beacon spot. If we ignore the cases in which we encountered a tracking problem the mean degradation in Strehl is 8.7%.

4.2. DM-Not-in-Pupil vs All-in-Pupil experiment

Moving an optical trombone shifts the position of the SM, the DM and the WFSs relative to the pupil allowing us to adjust the bench to the DNiP or AiP configuration. In this way we are

able to measure the degradation in Strehl as the DM is moved 1 km out of pupil. As previously discussed in the section 2 there are three main causes of degradation in Strehl in the $z_{DNI\bar{P}}$ plane. 1) magnification anisoplanatism, 2) Fresnel propagation of the wavefront, and 3) propagation of the existing degradation in focus anisoplanatism.

In the DNI \bar{P} configuration we measured the wavefront at SRI 2 and at the Hartmann WFSs which are both conjugate to the DM and ~ 1 km out of pupil. The AiP configuration places all WFSs and the DM conjugate to the pupil. A comparison of DNI \bar{P} vs AiP Strehl is essentially a comparison of data taken with the DM-WFS pair at pupil vs. DM-WFS out of pupil. As in the DNI \bar{P} data collection Strehl is determined by dividing the closed loop intensity by the true PSF.

The prerequisite for comparing DNI \bar{P} data with AiP data is that the atmospheric parameters for each configuration be the same. Meaning the r_0 , Rytov, and Greenwood frequencies should be identical. Though the atmospheric parameters were set to be the same the turbulence sensed by the DM would be different for the DNI \bar{P} and AiP cases due to the effective propagation of phase between the two scenarios. We compare the DNI \bar{P} science Strehl with the AiP science Strehl for 5 different cases. The data was collected between May 29 2007 and June 29 2007. The percent degradation in Strehl between the DNI \bar{P} and AiP cases is shown in Table 5.

Comparison of DNI \bar{P} 'vs' AiP Science Strehl					
WFS	May 29 DNI \bar{P}	June 20 DNI \bar{P}	June 20 DNI \bar{P}	June 29 DNI \bar{P}	June 29 DNI \bar{P}
	vs	vs	vs	vs	vs
	May 30 AiP	May 31 AiP	June 1 AiP	June 1 AiP	May 31 AiP
	(%)	(%)	(%)	(%)	(%)
Hart	2.77	13.44	10.92	0.80	3.60
SRI	6.36	16.37	14.45	6.32	8.32

Table 4. *The degradation in Strehl as a result of moving the DM-WFS pair 1 km out of pupil.*

The degradation in Strehl recorded as the DM-WFS is moved out of pupil is between 2 and 17% which is comparable to the 7 to 15% degradation predicted by wave optics simulations. As expected from our Fresnel Analysis (see appendix A and simulation results moving the DM 1 km out of pupil does not significantly effect the degradation in Strehl. Nevertheless we need to be cautious of these results since implementing a one-to-one comparison between DNI \bar{P} and AiP configurations is difficult. One has to be careful about setting the pupil iris to the same position when switching between configurations. One also has to ensure that the SRI 2 WFS moves with the pupil while the pupil is moved 1 km relative to the SRI 1 and the Hartmann WFSs.

5. MITIGATION TECHNIQUE

One experimental mitigation technique we tried compared the science Strehl at the pupil with the science Strehl at the $z_{DNI\bar{P}}$ plane while the DM was kept at the $z_{DNI\bar{P}}$ plane. The idea was

June 29 2007 Data — Lens set 6							
LWP = 16B, HWP = 16C, both PWs in pupil							
s PW rotation speed 5, 5							
$D_g = \frac{SRI\ 1\ bcn - SRI\ 2\ sci}{SRI\ 1\ bcn} * 100$				Statistics			
Case 1	Case 3	Case 5	Case 8	Mean $_{D_g}^{1,3,5,8}$	Std $_{D_g}^{1,3,5,8}$	Mean $_{D_g}^{3,8}$	Std $_{D_g}^{3,8}$
(%)	(%)	(%)	(%)	(%)		(%)	
3.12	8.74	-5.14	9.68	4.10	6.81	9.21	0.66
PW rotation speed 12, 12							
$D_g = \frac{SRI\ 1\ bcn - SRI\ 2\ sci}{SRI\ 1\ bcn} * 100$				Statistics			
Case 2	Case 4	Case 6	Case 7	Mean $_{D_g}^{2,4,6,7}$	Std $_{D_g}^{2,4,6,7}$	Mean $_{D_g}^{4,6,7}$	Std $_{D_g}^{4,6,7}$
(%)	(%)	(%)	(%)	(%)		(%)	
-8.45	-3.19	2.43	-2.41	-2.91	4.45	-1.30	3.31

Table 5. *This table shows the results of the experimental mitigation technique. The comparison of Strehl is done between the following two scenarios: scenario 1: WFS conjugate to pupil and DM not conjugate to plane and scenario 2: WFS-DM pair are at $z_{DNI\ P}$ plane.*

to mitigate the degradation in Strehl by moving only the DM out of pupil while keeping the WFS in pupil. The Strehl measured at the pupil WFS was compared to the Strehl measured at the WFS conjugate to the DM.

The experimental configuration to carry out the mitigation is that of DNI_P, i.e. the DM-SRI 1 WFS pair are conjugate to one another, ~ 1 km out of pupil, and in the $z_{DNI\ P}$ plane. The SRI 2 WFS is conjugate to the pupil. The beacon is measured at the SRI 1 and the science beam is measured at SRI 2 in a closed loop operation. The Strehl comparison between the two is shown in Table 5.

The results show that there is not much difference between moving the DM-WFS pair out of pupil or only moving the WFS out of pupil. The degradation actually seems to get worse when the WFS is conjugate to the pupil and the DM is conjugate to the $z_{DNI\ P}$ plane because now we are correcting in the $z_{DNI\ P}$ plane and applying the corrections to the science beam in the pupil plane. The mean Strehl degradation measured from Cases 3, 5, and 8 is 9.21 % for the mitigation scenario and it is 8.7 % for the DNI_P configuration.

6. CONCLUSION

The AFRL, SOR is in the process of developing a high efficiency AO system for its 3.5 m telescope. In order to increase the optical throughput the number of optics need to be reduced. A possible solution is to effectively place the DM 1 km behind the pupil. Wave-optics simulations show a 7 % to 15 % degradation in strehl as a result of moving the DM ~ 1 km out of pupil.⁶ We developed a lab experiment to test the degradation in Strehl and to implement a mitigation strategy.

We successfully carried out an experiment that demonstrates closed loop performance while the DM is not conjugate to the pupil. Due to opto-mechanical complications it was not trivial to move the DM-WFS pair in and out of pupil to compare the degradation in Strehl. However

we were able to effectively measure the degradation in Strehl as the DM was moved out of pupil. The degradation in Strehl is between 2 % and 17 % which is in accordance with wave-optics simulations.

The degradation in Strehl caused by moving the DM 1 km out of pupil is minute and therefore very difficult to measure within system error. Moving the pupil relative to the DM requires, moving the optical trombone, moving the pupil SRI WFS referred to as SRI 2, and resetting the pupil iris. This introduces errors and makes the in-pupil to out-of-pupil comparison arduous. Nevertheless we conclude that it is possible to carry out a closed loop experiment with DM placed not conjugate to the pupil. The mitigation strategy of placing the WFS at pupil while the DM was 1 km out of pupil does not recover the degradation in Strehl. Further mitigation techniques will be discussed in Part 2.⁷

APPENDIX A. FRESNEL PROPAGATION

In this experiment the in coming light instead of being measured at the aperture is propagated 1 km beyond the aperture where it is sensed by the WFS. According to the theory of Fresnel propagation as amplitude and phase are propagated they interchange into one another such that the resultant amplitude and phase measured a distance z from pupil will be different from the phase and amplitude measured at the pupil. In this section we explore the effect of Fresnel propagation on phase and amplitude as a function of Δz .

In Fresnel diffraction the observed field strength is found by taking the Fourier transform of the product of the aperture distribution $U(x_0, y_0)$ and the quadratic phase function $\exp\{i\frac{k}{2z}[(x_1 - x_0)^2 + (y_1 - y_0)^2]\}$. For a diffracting aperture in the (x_0, y_0) plane illuminated in the positive $z_{DNI P}$ direction the wave field a distance z away in the (x_1, y_1) plane is given by the Huygens-Fresnel Principle,¹¹

$$U(x_0, y_0) = \frac{e^{ikz}}{iyz} \int_{-l/2}^{l/2} \int_{-l/2}^{l/2} U(x_1, y_1) e^{i\frac{k}{2z}[(x_1 - x_0)^2 + (y_1 - y_0)^2]} dx_1 dy_1 \quad (1)$$

where $U(x_0, y_0)$ is the optical disturbance at the aperture, $U(x_1, y_1)$ is the optical disturbance at the target plane, k is the wave number given by $2\pi/\lambda$, and z is the distance between the aperture and the target which in our case is the DM.

The Fresnel number represents the number of fringes seen in the target plane and is inversely proportional to the distance to the target plane. The Fresnel number is given by,¹¹

$$N_F = \frac{w^2}{\lambda z} \quad (2)$$

where w is the aperture radius, and λ is the wavelength in question. The phase and intensity of the optical wave at the target plane can be determined if the optical disturbance at the target plane is known. The intensity is determined by taking the square of the absolute value of the optical disturbance at the target plane.

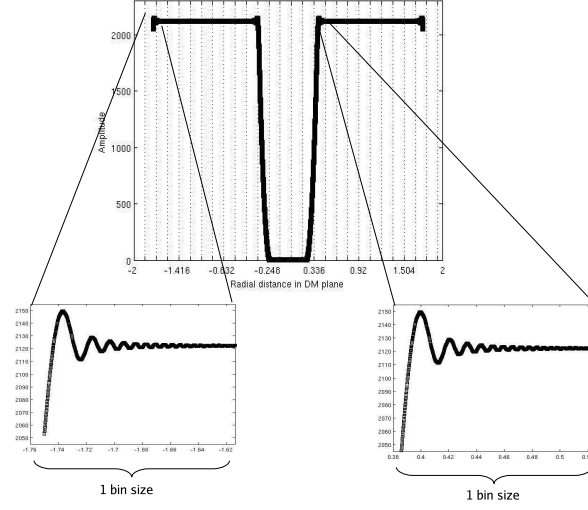


Figure 7. Fresnel propagated amplitude pattern for $\lambda = 589\text{ nm}$, aperture size $D_{outer} = 3.5\text{ m}$, and secondary size $D_{inner} = 0.595\text{ m}$. The inset shows the Fresnel ringing at the edges of the outer and inner apertures. Note that due to the high Fresnel number the fluctuation in amplitude per bin is minute.

We perform simulations for light of wavelength $\lambda = 589\text{ nm}$ that falls on a telescope with an aperture size $D_{outer} = 3.5\text{ m}$, and a secondary mirror of size $D_{inner} = 0.595\text{ m}$. The light is then Fresnel propagated $\Delta z \sim 1\text{ km}$ beyond the aperture to the DM plane. Fresnel numbers in the outer edges of the aperture are governed by the diffraction pattern from the 3.5 m aperture and those from the inner region are governed by the diffraction pattern of the 0.595 m central obscuration. The Fresnel number corresponding to D_{outer} is ~ 6499 and to D_{inner} is ~ 188 . We want to determine the effect of Fresnel propagation on the light beam. We expect the largest excursion in amplitude and phase fluctuation to be at the aperture edges. However even at the aperture edges the variation in intensity and phase is only about 1% and everywhere else is $\leq 1\%$. Figures 7 and 8 show the Fresnel propagated amplitude and phase with the insets showing the Fresnel ringing per bin for the amplitude and Fresnel ringing every 2 bins for the phase. Based on these plots we conclude that Fresnel propagation only accounts for less than 1% degradation in strehl.

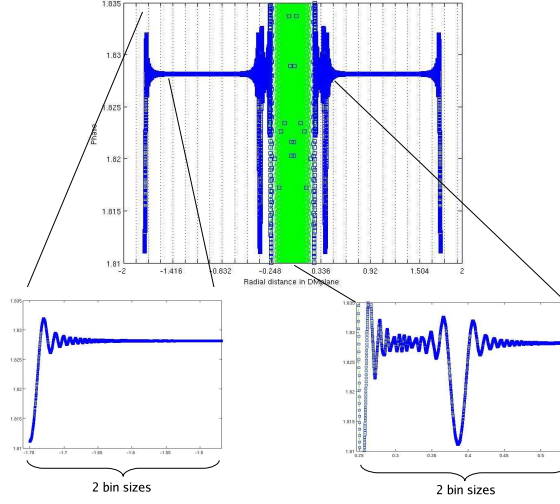


Figure 8. Fresnel propagated phase pattern for $\lambda = 589\text{ nm}$, aperture size $D_{\text{outer}} = 3.5\text{ m}$, and secondary size $D_{\text{inner}} = 0.595\text{ m}$. The inset shows the Fresnel ringing at the edges of the outer and inner apertures. Note that due to the high Fresnel number the fluctuation in phase over two bin sizes is minute.

REFERENCES

1. H. M. Martin, G. Brusa Zappellini, B. Cuerden, S. M. Miller, A. Riccardi, and B. K. Smith, “Deformable secondary mirrors for the LBT adaptive optics system,” in *Advances in Adaptive Optics II. Edited by Ellerbroek, Brent L.; Bonaccini Calia, Domenico. Proceedings of the SPIE, Volume 6272, pp. 62720U (2006).*, Presented at the Society of Photo-Optical Instrumentation Engineers (SPIE) Conference **6272**, July 2006.
2. F. P. Wildi, G. Brusa, A. Riccardi, M. Lloyd-Hart, H. M. Martin, and L. M. Close, “Towards 1st light of the 6.5m MMT adaptive optics system with deformable secondary mirror,” in *Adaptive Optical System Technologies II.*, P. L. Wizinowich and D. Bonaccini, eds., Presented at the Society of Photo-Optical Instrumentation Engineers (SPIE) Conference **4839**, pp. 155–163, Feb. 2003.
3. G. Brusa, A. Riccardi, P. Salinari, F. P. Wildi, M. Lloyd-Hart, H. M. Martin, R. Allen, D. Fisher, D. L. Miller, R. Biasi, D. Gallieni, and F. Zocchi, “MMT adaptive secondary: performance evaluation and field testing,” in *Adaptive Optical System Technologies II.*, P. L. Wizinowich and D. Bonaccini, eds., Presented at the Society of Photo-Optical Instrumentation Engineers (SPIE) Conference **4839**, pp. 691–702, Feb. 2003.
4. D. L. Miller, G. Brusa, M. A. Kenworthy, P. M. Hinz, and D. L. Fisher, “Status of the NGS adaptive optic system at the MMT Telescope,” in *Advancements in Adaptive Optics II.*, D. Bonaccini Calia, B. L. Ellerbroek, and R. Ragazzoni, eds., Presented at the Society of Photo-Optical Instrumentation Engineers (SPIE) Conference **5490**, pp. 207–215, Oct. 2004.
5. R. Arsenault, R. Biasi, D. Gallieni, A. Riccardi, P. Lazzarini, N. Hubin, E. Fedrigo, R. Donaldson, S. Oberti, S. Stroebele, R. Conzelmann, and M. Duchateau, “A deformable secondary mirror for the VLT,” in *Advances in Adaptive Optics II.*, Presented at the Society of Photo-Optical Instrumentation Engineers (SPIE) Conference **6272**, July 2006.

6. Personal communication: Dr. Barry Focoualt carried out wave optics simulations to determine the degradation in strehl for the DNIP geometry.
7. D. Sanchez, K. Lilevjen, T. Rhoadarmer, M. M., D. W. Oesch, D. Fung, P. Kelly, R. J. Vincent, R. A., and A. L. Petty, R., "Investigation of closed loop performance with deformable mirror out of pupil- paper 2: Mitigation of the degradation," 2008. To be presented at the SPIE Annual Conference in August 2008.
8. R. Q. Fugate *et al.*, "Experimental demonstration of real time atmospheric compensation with adaptive optics employing laser guide stars," *Bulletin of American Astronomical Society* **23**(2), p. 898, 1991.
9. R. Q. Fugate *et al.*, "Measurement of atmospheric wavefront distortion using scattered light from a laser guide-star," *Nature* **353**, pp. 144–146, 1991.
10. S. V. Mantravadi, T. A. Rhoadarmer, and R. S. Glas, "Simple laboratory system for generating well-controlled atmospheric-like turbulence," in *Advanced Wavefront Control: Methods, Devices, and Applications II. Edited by Gonglewski, John D.; Gruneisen, Mark T.; Giles, Michael K. Proceedings of the SPIE, Volume 5553, pp. 290-300 (2004).*, J. D. Gonglewski, M. T. Gruneisen, and M. K. Giles, eds., *Presented at the Society of Photo-Optical Instrumentation Engineers (SPIE) Conference 5553*, pp. 290–300, Oct. 2004.
11. J. W. Goodman, *Introduction to Fourier Optics*, McGraw-Hill, Boston, Mass., 1988 (first edition).

DISTRIBUTION LIST

DTIC/OCP 8725 John J. Kingman Rd, Suite 0944 Ft Belvoir, VA 22060-6218 1	1cy
AFRL/RVIL Kirtland AFB, NM 87117-5776	2 cy
Patrick Kelly Official Record Copy AFRL/RDSA	1 cy